

ON THE MECHANISM OF NONDESTRUCTIVE EVALUATION OF CEMENTITE CONTENT IN STEELS USING A COMBINATION OF MAGNETIC BARKHAUSEN NOISE AND MAGNETIC FORCE MICROSCOPY TECHNIQUES

L. Batista¹, U. Rabe^{1,2}, I. Altpeter¹, S. Hirsekorn¹, and G. Dobmann¹

¹*Fraunhofer Institute for Non-destructive Testing (IZFP), Campus E3 1, 66123
Saarbrücken*

²*University of the Saarland, LZPQ, 66123 Saarbrücken, Germany*

ABSTRACT. The influence of the carbon content in form of globular cementite precipitates in unalloyed steels was macroscopically characterized by means of magnetic hysteresis loop and Barkhausen noise techniques. The choice of the frequency of the applied field has a strong influence on the Barkhausen noise profiles. At sufficiently high frequency (0.5 Hz) there are two peaks, one at lower field, the amplitude of which corresponds to the amount of ferrite and one at higher field, the amplitude of which corresponds to the amount of the cementite phase, respectively. Magnetic force microscopy and electron backscattered diffraction techniques were used to determine the magnetic and crystallographic microstructures of the steels. Cementite has its own domain structure and stray fields which influence the magnetization process of the steel by its own magnetic contribution. When an external magnetic field is applied, the magnetization process in ferrite occurs mainly at lower fields through the 180° and 90° domain walls. A higher field is required for the observation of 180° domain wall movements in cementite.

Keywords: Magnetic force microscopy (MFM), Electron backscatter diffraction (EBSD), Steel, Magnetic domains, Barkhausen noise, Non-destructive testing

1. INTRODUCTION

In most steels, among all the phases or constituents that can be obtained by choosing the chemical composition and thermo-mechanical treatments, two are frequently encountered: ferrite and cementite. Ferrite shows high ductility and low strength values and therefore low mechanical and also - very often - magnetic hardness in terms of coercivity. Cementite on the other hand shows high mechanical and magnetic hardness and is much more brittle. Thus, the relative volume fraction of the ferrite and cementite phases gives rise to the final mechanical and magnetic properties of the steel. The knowledge of the amount of cementite in steels is thus crucial.

Hysteresis loop and magnetic Barkhausen noise (MBN) evaluations are widely used magnetic measurement techniques for the microstructural characterization of ferromagnetic materials and determination of residual stress states. In physics, regular hysteresis measurements providing reproducible and reliable results can only be performed by using special hystrometer measurement devices asking for specially shaped test specimens like spheres and cylinders with well-designed geometry combined with encircling coils to measure the magnetic induction. As a consequence the technique cannot be applied to real components, as for instance vessel shells or pipes or high speed running steel sheets in a cold rolling mill [1], and is therefore destructive. All techniques based on magnetic circuit approaches [2] suffer from influence of lift-off on absolute value, ensuing value fluctuations, and shearing of the hysteresis curve [3]. Only in case of transformer steel sheets industrial consensus standards exist (i.e. Epstein frame measurements [4]) basing on destructive batch tests. In contrast to these facts MBN-analysis can be performed with sensors positioned locally on top of the

surface of a component, which means that MBN is non-destructive. However, the use of the magnetic Barkhausen noise techniques is “not yet” regulated by a standard. This makes the comparison of results published by different authors extremely difficult, especially as the side influences of the different experimental conditions such as magnetization set-up, signal pick-up, band width, etc. are often insufficiently described. First attempts into standardization are initialized by the German Engineering Society (VDE Guidelines) [5].

During the magnetization process the domain structure of a ferromagnetic material is altered which involves different movements of the domain walls. There are exclusively 90°- and 180°- domain walls in case of iron materials. In the case considered here, the domain wall movement takes place in a microstructure consisting of a ferrite matrix with cementite precipitates. In basic physics the precipitates are either assumed acting as nonmagnetic foreign bodies [6,7] in the ferromagnetic matrix, or they are considered to interact with the domain walls of the matrix via their residual stress fields [8]. Domain walls tend to cling to nonmagnetic inclusions in order to minimize the magnetostatic and the wall energy. It was considered in the literature in a first approach that cementite behaves as a nonmagnetic inclusion in a ferrite matrix [9] or even as a nonmagnetic phase at all [10]. However, cementite is a ferromagnetic phase [11,12], and therefore – depending on its size, shape, crystalline orientation and amount of defects - it has its own domain structure and stray fields. The stray fields of inclusions, which are a source of magnetostatic energy, may also interact with the domain walls within the matrix. In order to reduce the magnetostatic energy, supplementary domains (closure domains) are built close to the inclusions which in turn interact with the domain walls in the matrix [13,14]. The other source of interaction of the cementite precipitates with the domain walls in the ferrite phase are – as mentioned above - the residual stresses which are built-up due to different thermal expansion coefficients of the two phases during the

solidification process of the material, and lattice defects, e.g. dislocations, which are created on the interface between ferrite and cementite.

Several studies have been done on the individual influence of different microstructural parameters, e.g. second phase particles, on the generation of the magnetic Barkhausen noise. For example, the observed MBN activity profile in a microstructure containing cementite in a ferrite matrix showed either a single [15] or a double peak [8,16]. The description of a double peak for a Barkhausen noise profile has also encountered divergences in the literature. The weaker field peak was attributed to the pinning of 180° walls in the matrix by secondary particles and the stronger field peak was explained by annihilation of 90° domain walls at grain boundaries [17]. Contrarily, *Moorthy et al* [16] state that the weaker field peak is caused by irreversible domain walls in the ferrite and the stronger field peak by irreversible movement of domain walls overcoming second phase particles. By measuring the MBN signal as a function of temperature of a compact cementite and unalloyed white cast iron samples, Altpeter [18] demonstrated that the cementite actively produces its own MBN signal. With increasing temperature the ferromagnetic coordination decreases, and consequently the MBN signal intensity decreases. The Curie temperature of cementite ($\sim 210^\circ\text{C}$) is lower than the Curie temperature of ferrite ($\sim 770^\circ\text{C}$). Altpeter observed a Barkhausen noise amplitude of the compact cementite specimen, which decreased with increasing temperature and disappeared at the Curie temperature of cementite [18]. Furthermore, the MBN amplitude of white cast iron showed qualitatively the same behavior, i.e. it decreased strongly towards the Curie temperature of cementite and remained at a low almost constant level above this value. In addition, the MBN decrease of white cast iron was stronger with increasing amount of cementite.

In this work, we investigate the opportunity of assessing the relative proportion and contributions of the cementite and ferrite phases in unalloyed steels by optimizing the measured

hysteresis loop and Barkhausen noise parameters. The evolution of the magnetic microstructure is directly correlated to the macroscopic measurement quantities by means of a superposed magnetic field applied to a Magnetic Force Microscope (MFM).

2. MATERIALS AND METHODS

Three different materials were examined in this study, a high purity iron (99.99%) and two unalloyed steels, Fe-0.8%C and Fe-1.5%C, containing globular cementite (Fe_3C) embedded in a ferrite matrix. The samples were provided as-cast and machined in a cylindrical shape of 8 mm diameter and 50 mm length. In order to remove all processing-induced residual stresses the samples were vacuum annealed at 600°C for 4h. The resulting microstructure has an average grain size of 80 μm for all samples. The size of the cementite precipitates ranges from a few hundred nanometers to about 10 μm in diameter.

The hysteresis loop and Barkhausen noise measurements were performed inside an electromagnet with a computer-controlled bipolar power supply (Fig. 1). The magnetic tangential field strength H was measured by a Hall probe. The cylindrical samples were magnetized along their axial direction up to a maximum magnetic field strength of 11000 A/m at different excitation frequencies of 0.05 Hz, 0.1 Hz and 0.5 Hz, respectively. The change in magnetic flux density B and the magnetic Barkhausen noise amplitude M were measured by a pick-up coil with 300 turns (wire diameter: 0.1 mm, resonance frequency: 710 kHz) surrounding the sample (Fig. 1). The envelope of the noise signals (analyzed frequency range $f_A = 200 \text{ Hz} - 50 \text{ kHz}$) and the magnetic flux density were recorded as a function of the tangential field strength.

Small specimens ($3 \times 3 \times 1 \text{ mm}^3$) were cut by spark erosion from the annealed cylindrical samples for the atomic force microscopy (AFM) and magnetic force microscopy investigations. The specimens were mechanically polished using standard procedures and

slightly etched using Nital (95% ethanol+5% nitric acid). The AFM and MFM techniques were used to image the topography and the magnetic microstructure of the samples, respectively. The measurements were performed in tapping-lift mode using a commercial AFM/MFM instrument (Nanoscope III[®] multimode, Bruker AXS Inc. (formerly Digital Instruments / Veeco), Madison, WI, USA). The sensor tips were CoCr-coated with a coercivity of ~ 32000 A/m (MESP, Bruker AXS Inc., Madison, WI, USA). The topography images show the local height of the sample surface displayed in grey scales. The magnetic images are taken by vibrating the AFM sensor at its resonance frequency at a predefined lift height above the sample surface. The gradient of the magnetic interaction forces cause a phase shift in the cantilever vibration which is displayed in grey scales. A lift-height of 60-100 nm was chosen for all measurements reported here. In order to investigate the evolution of the magnetic microstructure and the resulting domain configuration, an external electromagnet was combined with the MFM as shown in Fig. 2. The pole shoes of the electromagnet were adjusted such that the sample inside the AFM was magnetized parallel to its surface.

3. RESULTS AND DISCUSSION

3.1. BULK MAGNETIC PROPERTIES

The unalloyed steels investigated here consist of a relatively hard ferromagnetic phase (cementite) embedded in a soft ferromagnetic phase (ferrite). The different microstructural states lead to characteristic changes of the hysteresis loops and Barkhausen noise profiles as shown in Figs. 3.

Magnetic hysteresis curves of the three samples for three different frequencies f (0.05 Hz, 0.1 Hz, and 0.5 Hz, respectively) of the applied external field are shown as dotted lines in Figs. 3. The coercivity H_c and loss per cycle W increase with frequency and carbon content,

while the relative permeability at the coercive field H_c and the saturation magnetization B_S at 10000 A/m decrease with increasing frequency f of the applied magnetic field. This means that the material reacts magnetically harder with increasing frequency of the external magnetic field. In addition, the magnetic hardness increases as the carbon content increases. A summary of the measured parameters is given in Table 1.

With increasing amount of carbon in form of globular cementite precipitates in the ferrite matrix the pinning of the domain walls in the ferrite matrix is enhanced due to the presence of the cementite which acts as a foreign body, and by its stress fields. Furthermore, the cementite phase contributes to the increase of the magnetic hardness of the steel because cementite is magnetically harder than the ferrite [12]. The increase of the magnetic hardness with increasing frequency observed through the widening of the hysteresis loops is a well-known phenomenon in the case of conductive magnetic materials and it is attributed to eddy current losses [19,20,21], which depend not only on the excitation frequency but also on the material electrical conductivity σ , amplitude of the magnetic induction B , sample dimensions, and the size and arrangement of the domains [22,23].

The Barkhausen noise profiles for the three samples measured at the same three frequencies are shown as continuous lines in Figs. 3. The curves are remarkably different in their shape (single peak and double peak) and in their maximum amplitude values. In case of a double peak of the MBN one observes a higher maximum at a low excitation field value ($H_{cm,1}$) and a lower peak ($H_{cm,2}$) at a higher excitation field value, as shown schematically in Fig. 1c. The Barkhausen noise amplitude M_{max} increases with the magnetizing frequency for all three samples because the overlapping of random pulses increases as the number of pulses per unit time increases. The Barkhausen noise amplitude M_{max} of the high purity iron sample is significantly larger (for all measured frequencies) than the values of the Fe-0.8%C and Fe-1.5%C samples, respectively. In general, the addition of carbon causes a broadening of the

Barkhausen noise peak and a decreasing peak height. This fact can be explained by the influence of interstitial carbon atoms in the ferrite matrix and the intra- and intergranular cementite precipitates as already discussed in a previous work [12].

At very low magnetization frequency (0.05 Hz) the sample containing the higher amount of carbon (1.5 wt%) shows already the emergence of an additional peak $M_{\max,2}$ at higher fields (Fig. 3g). By increasing the frequency to 0.1 Hz the emergence of an additional peak $M_{\max,2}$ can also be seen for the sample containing less carbon, i.e. Fe-0.8%C, and for the sample Fe-1.5%C the additional peak becomes more evident (Fig. 3e and h). At 0.5 Hz, the signals obtained for the samples containing carbon become clearly double-peak (Fig. 3f and i) while for the high purity iron still a single peak is observed (Fig. 3c). For the Fe-0.8%C and Fe-1.5%C samples where a double peak is observed, the amplitudes of the peaks seem to be proportional to the amount of carbon. With increasing amount of carbon, the peak amplitude $M_{\max,1}$ decreases and the peak amplitude $M_{\max,2}$ increases (Fig. 4). The results confirm that the weaker field peak $H_{\text{cm},1}$ corresponds to the ferrite and that the emergence of a second stronger field peak $H_{\text{cm},2}$ is related to the presence of the second (cementite) phase.

It is evident that the Barkhausen noise amplitude M_{\max} increases with magnetizing frequency f due to the faster transition between magnetic states, i.e., there is an increase of the number of pulses per unit time. Cementite is in a minor relative proportion compared to the ferrite in the unalloyed steel samples. To observe the contribution of the cementite on the MBN signal a minimum excitation frequency of the applied field and/or minimum cementite content are required. This explains the reason why for the sample containing higher amount of carbon (1.5 wt%) the signal of the cementite phase can already be observed at very low magnetizing frequency (0.05 Hz), while for the sample containing less carbon (0.8 wt%) a higher magnetizing frequency is necessary for the observation of the signal of the cementite phase.

The larger Barkhausen noise amplitude M_{\max} found for the high purity iron sample at all measured frequencies is attributed to the easy irreversible motion of domain walls (mostly 180° BWs) in the annealed pure iron with its low dislocation density and generally low density of lattice defects. In contrast, within the Fe-0.8%C and Fe-1.5%C samples, the 180° and 90° BWs in the ferrite interact with the cementite precipitates and with the interstitial carbon atoms in the ferrite matrix - as already mentioned above.

It was also reported [24] that the appearance of a second peak can be attributed to a uniaxial compressive stress. In our case, this argument can be excluded, because residual stresses, if still present in the investigated annealed samples, should be rather tensile stresses which would be built up during solidification due to the higher thermal expansion coefficient of ferrite in comparison to cementite. Another observation that supports the assumption that the stronger field peak $H_{\text{cm},2}$ is a signature of the cementite phase, is provided by the measurement of the temperature dependence on the MBN signal for example in the reactor pressure vessel steel DIN 22 NiMoCr 37 (ASTM A 508 Grade 2) containing globular and rod-shaped cementite. At room temperature, a double peak was observed in the MBN signal. After heating the sample up to the Curie temperature of the cementite ($\sim 200^\circ\text{C}$), the stronger field peak $H_{\text{cm},2}$ of the MBN signal disappeared [8].

It is well known that, in addition to the excitation frequency f , the analyzed noise frequency range f_A can strongly influence the amplitude of the Barkhausen noise signal. *Altpeter* [8] reported that the higher noise signal is obtained at high analyzing frequency, i.e. at $f_A = 50$ kHz, for a compact cementite sample and at lower analyzing frequency, i.e. $f_A = 1$ kHz, for an alloyed soft iron (AME1) sample, respectively. In order to obtain the highest noise signal for both phases, ferrite and cementite, all noise signals in this work were analyzed in a frequency range from 0.2 kHz to 50 kHz.

3.2 MFM IMAGES OF THE UNALLOYED STEEL SAMPLES CONTAINING GLOBULAR CEMENTITE EMBEDDED IN A FERRITE MATRIX

A detailed investigation of the magnetic microstructure while an external magnetic field is applied, allows a better understanding of the correlation of domain wall dynamics and magnetic hysteresis loop and Barkhausen noise profiles. The microscopic observation of easy reversible and irreversible domain wall movements in bulk pure iron [25,26] as well as the observation of pinning of domain walls by cementite precipitates in unalloyed steels [12,27] were previously reported. In this work the basic behavior of the magnetic microstructure with special emphasis to the processes related to the cementite is discussed by taking Fe-1.5%C as an example.

3.2.1 Domain wall dynamics in ferrite

Fig. 5a shows the topography obtained with the MFM of the Fe-1.5%C sample revealing three ferrite grains (numbered (1), (2), and (3)) with different average height and crystalline orientation. The evolution of the magnetic microstructure under influence of a superposed external magnetic field is shown in Figs. 5b, c and d. Fig. 5b is recorded in the demagnetized state of the sample while Figs. 5c and d display the results with an applied magnetic field of 19000 A/m and -19000 A/m, respectively. The cementite precipitates show a much stronger magnetic image contrast than the ferrite matrix because cementite is magnetically harder than ferrite and thus causes stronger stray fields.

Within the ferrite matrix, bright and dark lines which can be identified as domain walls are visible. In ferrite, the directions of easy magnetization [100] induce two types of walls: 90° and 180° Bloch walls. Curved 180° Bloch walls (arrows #4 and #5) are visible on grain (2). Branch domains [14] (arrow #3) and spike domains [13,28,29] (arrow #1) are

observed in grain (1). Such domains are typically enclosed by 90° walls. They are often bounded by main domains as for example the spike domains (arrow #1), which are bounded by the domains within a cementite precipitate. A supplementary domain [30] (arrow #2) is observed on grain (1). When applying a field of 19000 A/m to the left (Fig. 5c), the supplementary domain (#2) decreases its size, while the spike domain attached to the precipitate (#1) increases its size. The opposite is observed when a field of 19000 A/m is applied to the right (Fig. 5d), i.e. the supplementary domain increases its size at the expense of the area enclosed by the spike domain attached to the precipitate. Additionally, the two-arms branch domain (arrow #3) becomes nearly a single arm and the 180° BWs marked with the white arrows #4 and #5 are moved and bent, respectively, oppositely and into to the direction of the field. The results show that in ferrite both, the 90° and 180° BWs, move at relatively low applied fields while the domain structure in cementite remains unmodified.

3.2.2 Domain wall dynamics in cementite

Fig. 6a shows the topography obtained with the MFM and the corresponding electron backscatter diffraction map (Fig. 6b) taken in the same area with a scanning electron microscope, i.e. the inverse pole figure (IPF), of a section of grain (1) and (2) in Fig. 5. The color code of the inverse pole figure represents the crystallographic orientation in the ferrite matrix (nearly pure b.c.c. iron, lattice constant $a = 2.87\text{\AA}$), and in the cementite particles (orthorhombic symmetry, length of the three perpendicular axes $a = 5.09\text{\AA}$, $b = 6.74\text{\AA}$, $c = 4.52\text{\AA}$). The IPF map reveals that some cementite precipitates observed in the topography image (Fig. 6a) are not single crystals, but have a polycrystalline structure with different grain orientations. The cementite precipitate (Figs. 6b and 8) oriented in or around the (010) plane displays a domain structure composed of parallel stripes having opposite phase contrasts. This configuration suggests that the magnetic moments are positioned alternately down- and

upwards in relation to the surface and separated by 180° domain walls. It is also observed that the parallel stripes in the magnetic microstructure of the cementite oriented in or around the (010) plane are often branched, i.e. individual domains terminate within the cementite particle (as shown for example in Fig. 5b, arrows #6). The formation of the branched magnetic structure may be explained due to the accumulation of dislocations. In order to analyze the dislocation density in cementite, a thin foil of the Fe-0.8%C sample was examined by transmission electron microscopy (TEM). Using the focused ion beam technique, the thin foil was prepared such that a cementite precipitate was in the field of view of the TEM. The TEM micrograph in Fig. 7 visualizes dislocations in the cementite precipitate some of which seem to nucleate at the edge of the interface boundary between the cementite and ferrite. It was reported [31,32] that the domain wall configurations can be affected by the presence of dislocations. This occurs mainly because their internal stresses may cause a local deflection of the spins which leads to significant deviations from the saturated configuration.

Due to the very high anisotropy of the cementite its magnetic moments are not easily oriented by an applied magnetic field. Therefore, a higher magnetic field must be applied in order to observe domain wall movement in cementite. A higher field was reached by placing the pole shoes of the external electromagnet which is combined with the MFM (Fig. 2) closer to each other.

A cementite precipitate (selected area, Fig. 6b) oriented close to the (010) plane and therefore having the magnetic moments more or less positioned alternately down- and upwards in relation to the surface was chosen for further investigation using MFM with a strong superposed magnetic field. The evolution of the magnetic microstructure in the selected area (Fig. 6b) is shown in Figs 8. The weaker contrast compared to the MFM images in Figs. 5 is due to an increased lift-height during the MFM scanning process. Fig. 8a is recorded in the demagnetized state while Figs. 8b and c display the results with an applied magnetic field of

22000 A/m and 24000 A/m, respectively. The MFM line scans highlighted by white dotted lines in Figs. 8 and a respective qualitative model describing the interaction between the magnetic tip and the magnetic moments of the cementite are shown in Figs. 9. Since the MFM tip senses the component of the stray field emerging perpendicularly from the surface, we may conclude that in the demagnetized state the magnetic moments of the precipitate are more or less parallel to the tip axis, i.e. perpendicular to the sample surface plane (Figs. 8a and 9a). When applying a field of 22000 A/m to the left, the domains become wider because the magnetic moments start to rotate into the direction of the field, i.e. into the surface plane (Figs. 8b and 9b). By increasing the field to 24000 A/m the domains become even wider as shown in Figs. 8c and 9c. At this point, the magnetic moments are already almost aligned to the direction of the field in the surface plane. This results in a very weak image contrast in MFM comparable to that one in the ferrite matrix. In order to prove that when applying an external field the change in the contrast of the MFM images is due to the change in the magnetic state of the cementite precipitates and not due to changes in the magnetic tip, the experiment was repeated using a commercial hard disc sample with high in-plane coercivity (about 135000 A/m). When applying a field of 24000 A/m no change in the magnetic contrast was observed which confirms that there was no modification in the magnetic state of the tip due to the external field.

SUMMARY AND CONCLUSIONS

The dependence of the amount of carbon in form of globular cementite precipitates in unalloyed steels was macroscopically characterized by measuring hysteresis loops and Barkhausen noise signals. The magnetic hardness increases with the carbon content and the frequency of the applied magnetic field, which is explained by the enhanced pinning effect of the cementite precipitates and their stress fields, and by increasing eddy current losses at higher frequency, respectively.

For the Barkhausen noise the choice of the frequency of the applied field plays a crucial role in the detection of the cementite phase and for the nondestructive evaluation of its proportion in the unalloyed steels. With increasing amount of cementite, the Barkhausen noise profile exhibits a second maximum $M_{\max,2}$, however the emergence of the second peak becomes clearer with increasing frequency. Cementite is in a minor relative proportion compared to the ferrite phase, therefore a minimum excitation frequency of the applied field and/or a minimum cementite content are necessary to separate the contribution of the cementite in the MBN signal. The ferrite and cementite phases in the Fe-0.8%C and Fe-1.5%C samples were clearly recognized on the Barkhausen noise profiles measured at 0.5 Hz. The weaker field peak $H_{\text{cm},1}$ corresponds to the ferrite and the stronger field peak $H_{\text{cm},2}$ to the cementite phase.

The combination of AFM, MFM, and EBSD techniques enables the direct observation of magnetic micro- and nanostructures including the corresponding single crystal grain orientations. The AFM and MFM techniques were shown to be a powerful tool for topography imaging and magnetic micro- and nanostructure characterization of steels. The crystalline orientation of the cementite phase was determined by EBSD and correlated to the domain structure. Furthermore, using the TEM technique, dislocation structures were observed mostly in the cementite phase and in the interface between ferrite and cementite.

In this work, MFM images with a local resolution of 50 nm reveal that the cementite is ferromagnetic and that its stray fields are generally stronger compared to the ones of ferrite. The cementite has its own domain structure, and in order to reduce its magnetostatic energy, supplementary domains are often observed at the interface between the cementite precipitates and the ferrite matrix.

When an external field of 19000 A/m is applied, the position of the 180° and 90° DWs in the ferrite matrix change, while the domains in the cementite remain unmodified. This means that both, 180° and 90° BWs in ferrite, are moved at relatively low applied field. The 180°

domain walls are mainly situated in the center of the grains whereas the 90° domain walls are mainly observed in connection with the closure domains in proximity to the phase and grain boundaries. A change in the domain configuration of the cementite phase is observed only when a higher external magnetic field (22000 A/m) is applied. A larger field is required to move the domain walls in cementite due to its very high anisotropy and high density of defects, e.g. dislocations, which make the cementite magnetically harder than ferrite. The macroscopic measurements have shown that a field of 11000 A/m is strong enough to saturate all three samples. In our case the macroscopic magnetic measurements were performed with cylindrical samples, while the samples for MFM measurements were small square plates cut from the macroscopic cylinders. The different sample geometries and the fact that the MFM analysis relies on the behavior of surface domains, may explain the fact, that the field which had to be applied to move the domain walls in cementite was larger compared to the field which was necessary to reach saturation in the macroscopic measurements. The microscopic observation that a higher magnetic field is required to magnetize the cementite precipitates compared to ferrite correlates qualitatively with the increase of magnetic hardness with increasing amount of cementite and with the emergence of a second peak $M_{\max,2}$ in the Barkhausen noise signal at higher field which corresponds to the cementite phase.

ACKNOWLEDGMENTS

We thank K. Szielasko and members of the materials characterization department at Fraunhofer IZFP for interesting and helpful discussions. We gratefully acknowledge support from different chairs at the University of the Saarland, Saarbrücken, Germany: J. Schmauch, Technical Physics, helped with the EBSD measurements. The external coil for applying the

magnetic field in the MFM was provided by the chair for Experimental Physics, Nanostructural research and Nanotechnology, U. Hartmann.

REFERENCES

- [1] G. Dobmann, “State of the art to NDT for characterizing properties in the production of flat steel products”. In: Joint Seminar of the German Iron and Steel Institute (VDEh) and the German Society for NDT (DGZfP) in Düsseldorf to “Material Properties Determination”, Proceedings (in German) DGZfP Berlin (1999).
- [2] G. Bosse.: *Grundlagen der Elektrotechnik II – Das magnetische Feld und die elektromagnetische Induktion*; Mannheim: Hochschultaschenbücher (1967).
- [3] D.C. Jiles, J.B. Thielke, *Theory of ferromagnetic Hysteresis: Determination of Model Parameters from Experimental Hysteresis Loops*, IEEE Transactions on Magnetics **25** (1989).
- [4] H. Czichos, T. Saito, L. Smith (Eds.): *Springer Handbook of Materials Measurement Methods*; Leipzig: Springer (2006). p. 502-503.
- [5] VDI/VDE – Richtlinie 2616, Blatt 1, *Härteprüfung an metallischen Werkstoffen*, Düsseldorf: VDI (2012) s. 30-35.
- [6] M. Kersten, *Grundlagen einer Theorie der ferromagnetischen Hysterese und der Koerzitivkraft*, S. Hirzel, Leipzig (1943).
- [7] E. Kneller, *Ferromagnetismus*, Springer, Berlin (1962).
- [8] I. Altpeter, *Spannungsmessung und Zementitgehaltsbestimmung in Eisenwerkstoffen mittels dynamischer magnetischer und magnetoelastischer Meßgrößen*, Dissertation, Saarland University, Saarbrücken (1990).
- [9] L. J. Dijkstra and C. Wert, *Physical Review* **79** (1950), 979.
- [10] D.W. Kim and D. Kwon, *Journal of Magnetism and Magnetic Materials* **257** (2003) 175.

- [11] A. S. Keh, C. A. Johnson, *Journal of Applied Physics* **34** (1963) 2670.
- [12] L. Batista, U. Rabe, S. Hirsekorn, "Magnetic micro- and nanostructures of unalloyed steel: Domain wall interactions with cementite precipitates observed by MFM". *NDT&E Int* (2013), <http://dx.doi.org/10.1016/j.ndteint.2013.03.004>.
- [13] L. Néel, *Cahiers de Physique* **25** (1944) 21.
- [14] B. D. Cullity, *Introduction to magnetic materials*, Addison Wesley, London (1972).
- [15] M. Blaow, J.T. Evans, B.A. Shaw, *Acta Materialia* **53**, (2005) 279.
- [16] V. Moorthy, S. Vadyanathan, T. Jayakumar, B. Raj, *Journal of Magnetism and Magnetic Materials* **171** (1997) 179.
- [17] J.A. Pérez-Benitez, J. Capó-Sánchez, J. Anglada-Rivera, L.R. Padovese, *Journal of Magnetism and Magnetic Materials* **288** (2005) 433.
- [18] I. Altpeter, *Journal of Nondestructive Evaluation* **15** (1996) 45.
- [19] G. Bertotti, *J. Appl. Phys.* **54**, 5293 (1983).
- [20] G. Bertotti, *J. Appl. Phys.* **55** 4339 (1984).
- [21] D. C. Jiles, *J. Appl. Phys.* **76**, 5849 (1994).
- [22] D. Goll, *Handbook of Magnetism and Advanced Magnetic Materials*, Vol 2: Micromagnetism, ed. by H. Kronmüller, S. Parkin Wiley & Sons, New York (2007) pp.1047.
- [23] G. Bertotti, Magnetic losses, In *Encyclopedia of Materials: Science and Technology*, ed. by K.H.J. Buschow, R.W. Cahn, M.C. Flemings, et al., Elsevier, (2006) 4798.
- [24] A. Vincent, L. Pasco, M. Morin, X. Kleber, M. Delnondedieu, *Acta Materialia*, **53** (2005) 4579.
- [25] W. Drechsel, *Zeitschrift für Physik*, **164** (1961) 324–329.
- [26] L. Batista, U. Rabe, S. Hirsekorn, "Characterization of the magnetic micro- and nanostructure in unalloyed steels by Magnetic Force Microscopy", *39th Annual Review of*

Progress in Quantitative Nondestructive Evaluation (QNDE), Denver, Colorado, USA, July 16-20, 2012.

[27] S. Wust, *Untersuchung der magnetischen Domänen in Stahlproben mittels Magnetkraftmikroskopie unter Anlegen eines externen Magnetfeldes*, Diploma thesis, Saarland University, IZFP report No.110126-TW, Saarbrücken (2011).

[28] H. J. Williams, *Physical Review* **71** (1947) 646.

[29] H. Träuble, *Moderne Probleme der Metallphysik*, Bd. 2; Ed. by A. Seeger, Berlin-Heidelberg-New York (1966), pp. 238-255.

[30] A. Hubert, R. Schäfer, *Magnetic Domains - The Analysis of Magnetic Microstructures*, Springer, Berlin (1998).

[31] Ö. Özdemir, D.J. Dunlop, *Journal of Geophysical Research* **102** (1997) 20,211.

[32] J. N. Chapmann, *Journal of Physics D: Applied Physics*, **17** (1984) 623-647.

Measured parameter	Magnetization frequency [Hz]	Carbon content [wt%]		
		0 (Pure Fe)	0.8	1.5
Coercive field H_C [A/m]	0.05	240	470	660
	0.1	270	510	690
	0.5	420	680	820
Relative permeability μ_r	0.05	1700	1050	341
	0.1	1245	900	312
	0.5	746	490	294
Saturation magnetization B_S [T]	0.05	1.99	1.79	1.58
	0.1	1.99	1.78	1.57
	0.5	1.96	1.75	1.55
Loss per cycle W [mJ/kg]	0.05	2.76	5.08	6.38
	0.1	2.82	5.53	6.71
	0.5	4.40	6.33	7.18

Table 1: Parameters deduced from the macroscopic measurements shown in figures 3.

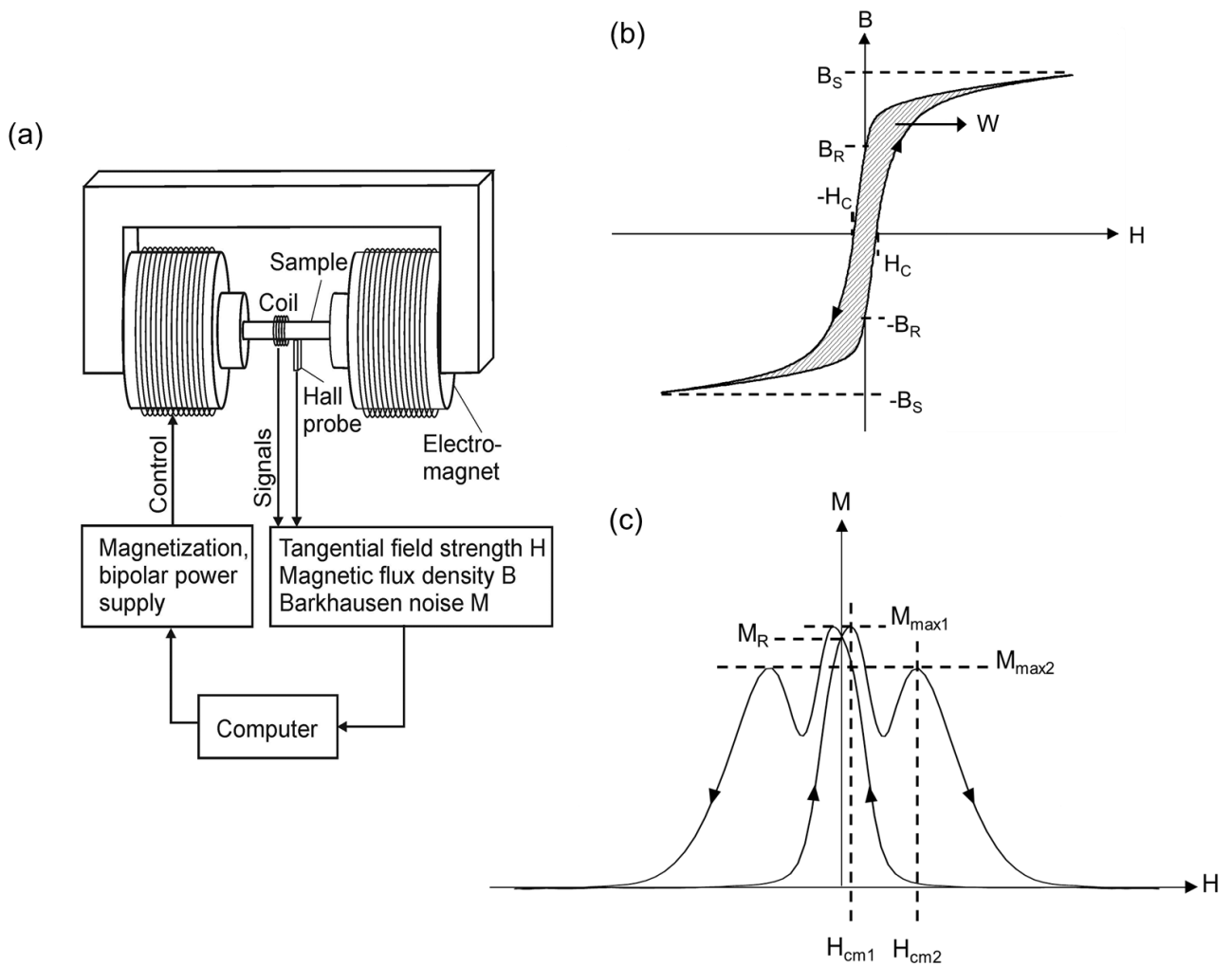


Figure 1. (a) Schematic sketch of the experimental set-up for hysteresis loop and Barkhausen noise measurements, (b) schematic hysteresis loop with coercive field H_C , magnetic flux at saturation B_S , remnant magnetic flux B_R , and loss per cycle W , (c) schematic Barkhausen noise curve with maximum amplitudes $M_{max1,2}$, remnant Barkhausen noise amplitude M_R , and coercive field $H_{cm1,2}$ deduced from Barkhausen noise curve.

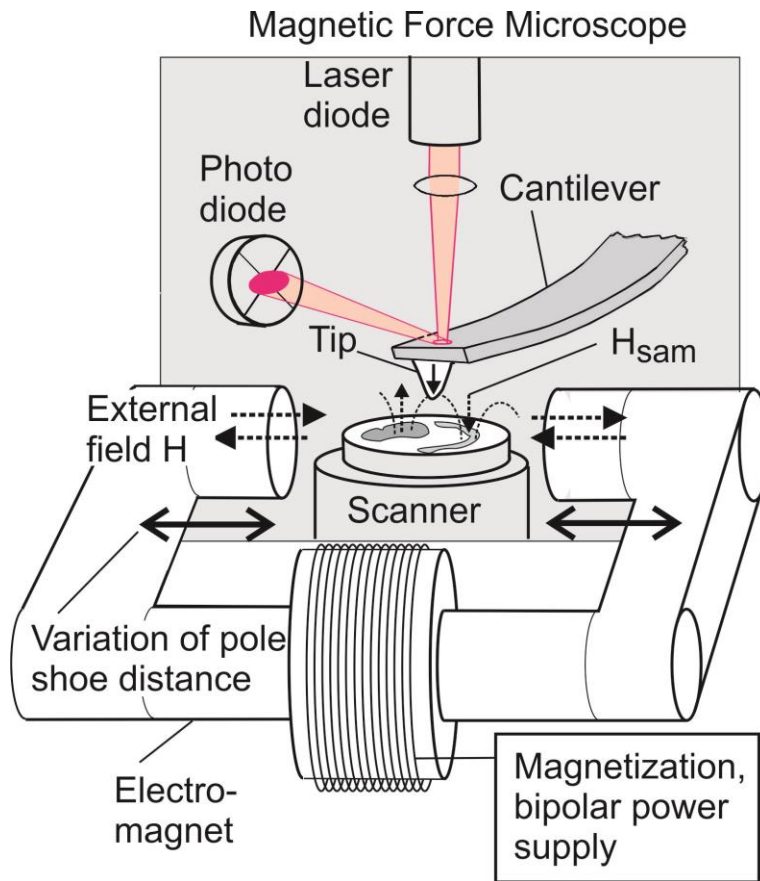


Figure 2. Experimental set-up for the MFM measurements coupled with an external coil providing a controlled external in-plane magnetic field. The strength of the field can be adjusted by the current applied to the coil and/or the distance of the pole shoes with respect to the sample.

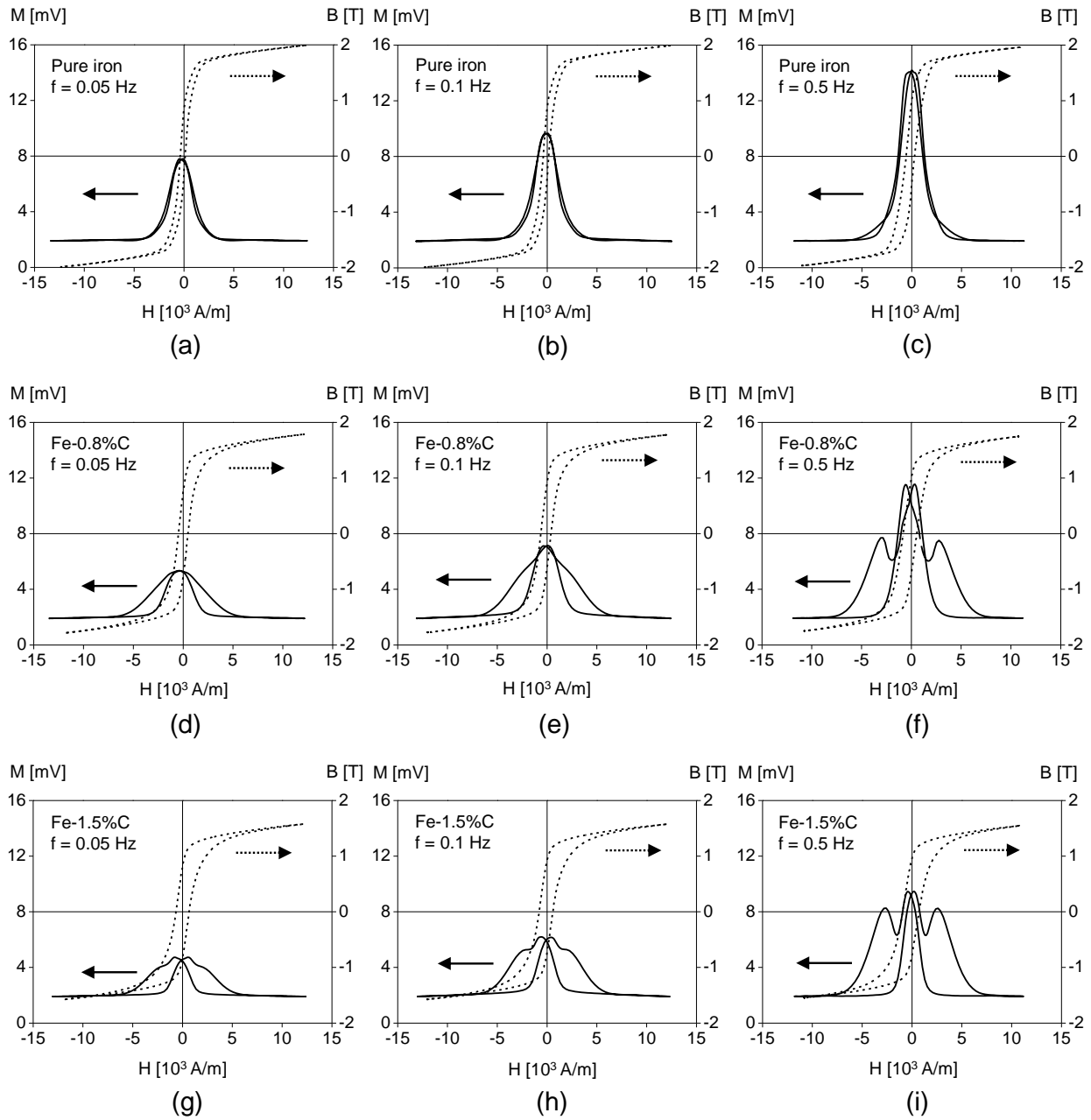


Figure 3: Hysteresis loop (dotted line) and Barkhausen noise (continuous line) curves for different oscillation frequencies of the applied external field recorded at pure Fe (99.99%) (a), (b) and (c) and at two unalloyed steels containing a different content of globular cementite, i.e. Fe-0.8%C (d), (e) and (f) and Fe-1.5%C (g), (h) and (i), respectively. The measurements were performed at 1.8 V and at frequencies of 0.05 Hz, 0.1 Hz and 0.5 Hz.

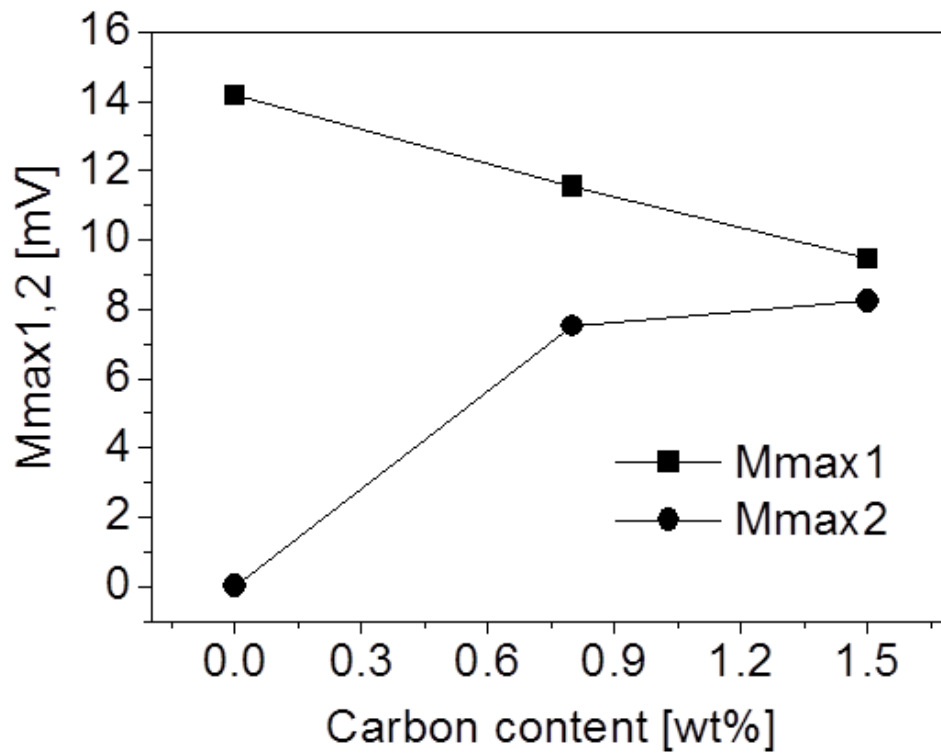


Figure 4: Maximum Barkhausen noise amplitude $M_{\max 1,2}$ as a function of carbon content for the pure Fe (99.99%), Fe-0.8%C and Fe-1.5%C samples. The measurements were performed at an excitation amplitude of 1.8 V and an excitation frequency of 0.5 Hz.

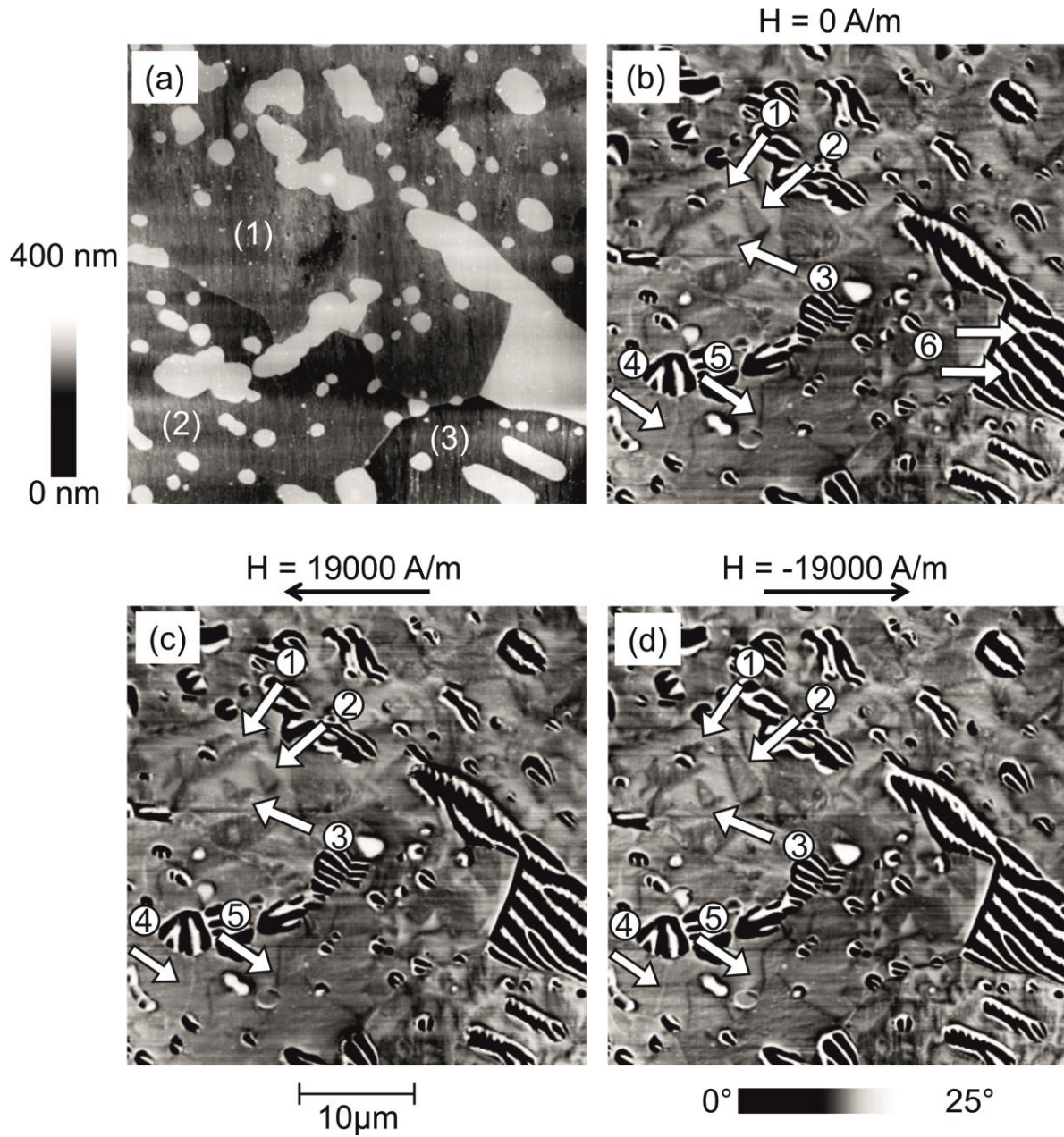


Figure 5: Topography (a) of the sample Fe-1.5%C containing globular cementite precipitates in a ferrite matrix. The grey scale covers a height range of 0 nm (black) to 400 nm (white). (b) MFM images taken without external magnetic field and with an applied field of (c) 19000 A/m and (d) – 19000 A/m, respectively. The direction of the in-plane field is indicated by black arrows. The grey scale of the MFM images covers a relative variation of the phase shift of 0° (black) to 25° (white).

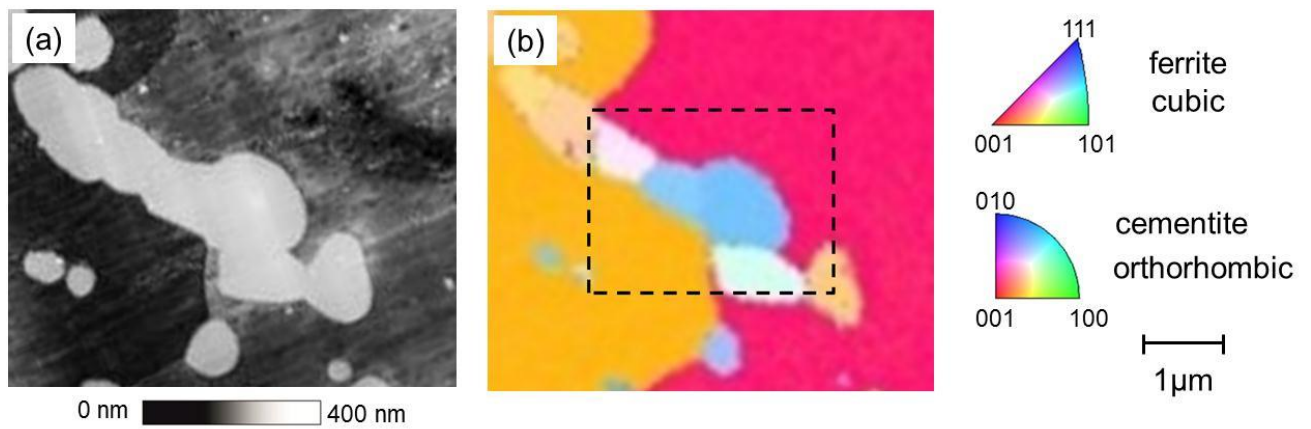


Figure 6: Enlarged section of figure 5a showing the topography (a) taken with the MFM. The corresponding IPF map taken in the same area with SEM shows the crystals and their respective orientations. The selected area was further measured by MFM, see Fig. 8.

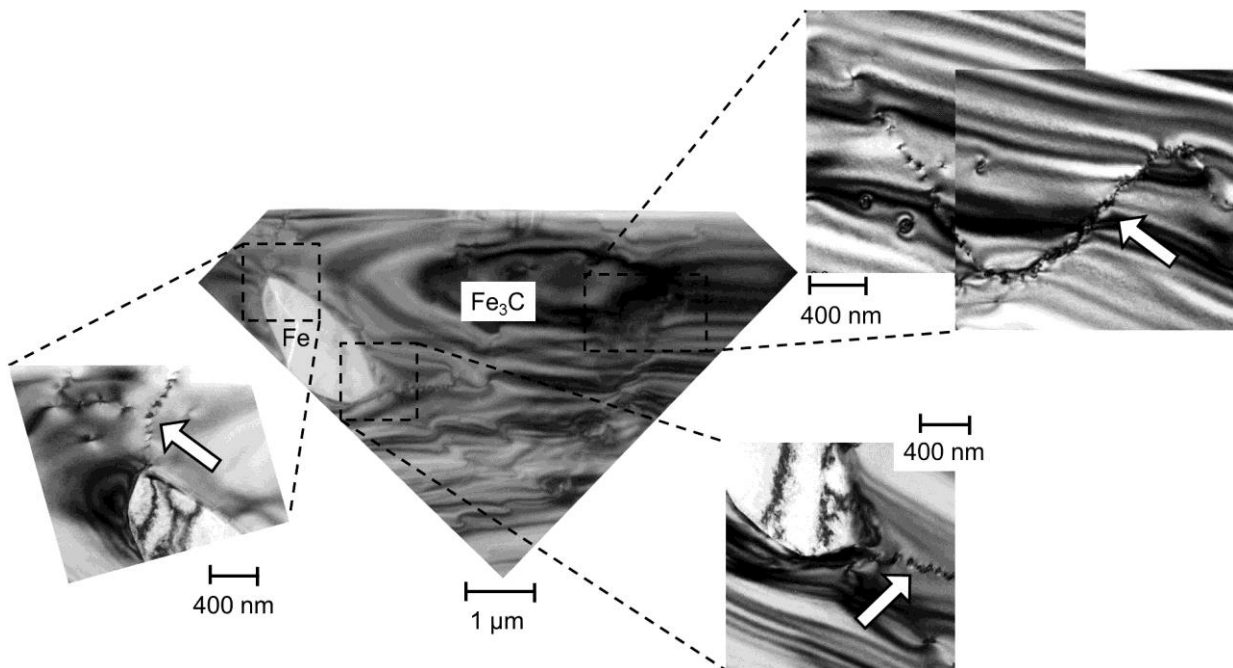


Figure 7: TEM images taken on a thin foil which was obtained from the Fe-0.8%C sample by cutting a cementite precipitate using the Focused Ion Beam (FIB) technique. A ferrite grain (in

light grey) surrounded by cementite is visible. The TEM micrographs show a rippled background contrast, which is probably due to the inhomogeneous thin foil thickness. The contrast obtained from the dislocations (see e.g. white arrows) is still clearly visible.

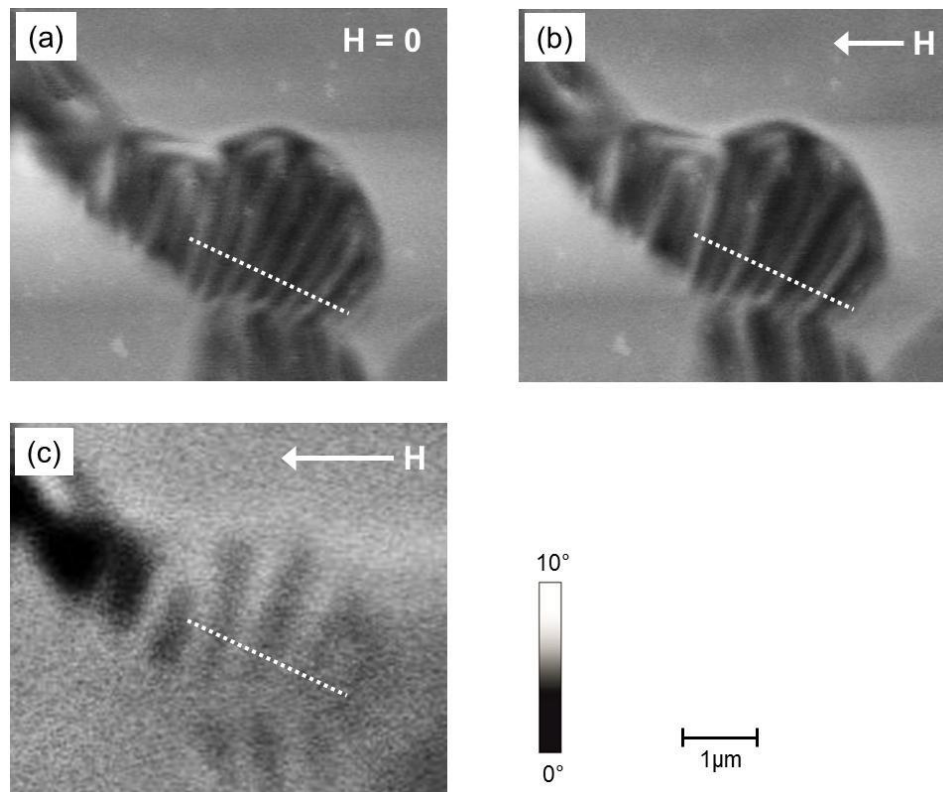


Figure 8: MFM images taken on the cementite precipitate in the selected area of Fig. 7b; (a) without external field; (b) and (c) with external fields of (b) 22000 A/m and (c) 24000 A/m, respectively. The applied field direction is indicated by the white arrows.

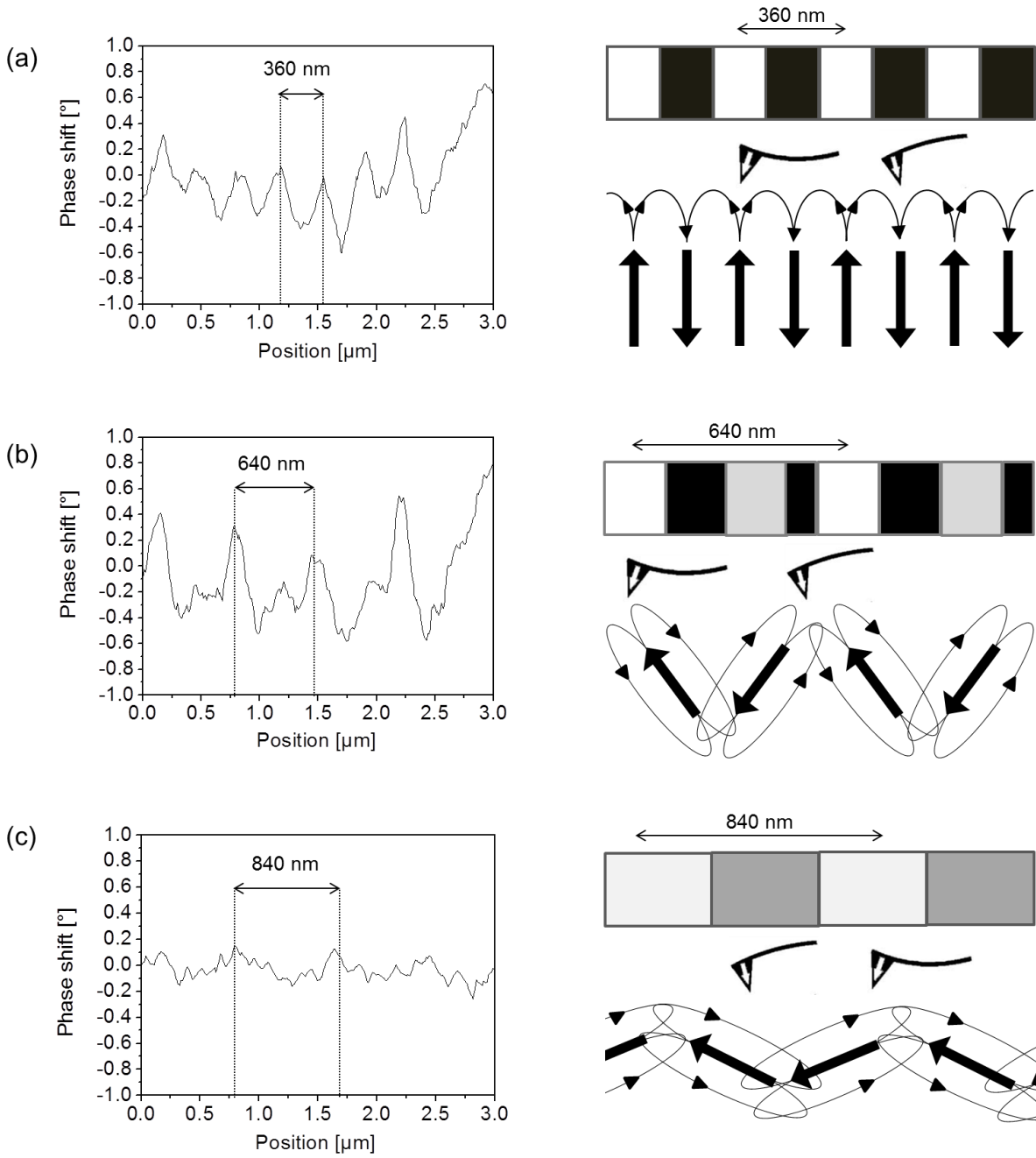


Figure 9: MFM line scans across the cementite precipitate (lines indicated in Fig. 8) together with a schematic model showing the interaction of the magnetic tip with the stray fields of the magnetic moments of the cementite and the respective obtained image contrasts (a) without external field and with external fields of (b) 22000 A/m and (c) 24000 A/m, respectively.